ASN.2015111224, 2016"
which should be cited to refer to this work.

Supplemental material

Functional Measurements

To study renal excretion, mice were placed in metabolic cages for two days on control diet (C1000, Altromin, Lage, Germany) and tap water. Urinary creatinine and serum urea were measured using enzymatic colorimetric creatinine and urea kits (Lehmann, Berlin, Germany), Urinary albumin was measured using a fluorimetric albumin test kit (Progen, PR2005, Heidelberg, Germany) following the manufacturer´s instructions. Evaluation of albuminuria (expressed as the albumin to creatinine ratio) was performed as previously described [1]. Plasma concentrations of Na^+, K^+ and Ca^{2+} were measured by flame photometry (efux 5057, Eppendorf, Hamburg, Germany). Plasma and urinary magnesium and phosphorus concentration were determined by colorimetric methods (Lehmann, Berlin, Germany).

Urinary and plasma HPLC measurements

Amino acid concentrations in plasma and urine were determined on Biochrom 30+ amino acid analyzers (Laborservice Onken, Gründau, Germany), using cation exchange chromatography and post-column derivatization with ninhydrin. Prior to injection, samples were deproteinized with sulfosalicylic acid. External control was performed using the ERNDIM quality control scheme (www.erndimqa.nl) "Amino Acids".

Fixation and tissue processing for immunohistochemistry and immunoblotting

Kidneys were shock-frozen for biochemical evaluation or perfused retrogradely using 4% PFA in PBS and either postfixed o/n and subsequently transfered into 0.1% PFA in PBS for

paraffin embedding or processed for electronmicroscopy or transferred into 800 mOsm Sucrose in PBS overnight and subsequently frozen in OCT. Paraffin embedded sections were further processed for PAS-staining. To assess fluid phase and receptor mediated endocytosis HRP (Sigma, Schnelldorf, Germany) was given at a concentration of 120µg/g BW and Alexa555 (Invitrogen, Karlsruhe, Germany) labeled ß-lactoglobulin (Sigma) at 4µg/g BW i.v. into the retroorbital plexus under light isoflurane anesthesia. Kidneys were harvested 5 min later and immediately perfused with 4% PFA in PBS and processed as described above. For electron microscopy tissue specimens were post-fixed in 1.5% glutaraldehyde and embedded in Epon 812 (Serva, Heidelberg, Deutschland) followed by contrasting ultrathin sections with osmium and uranylacetate. For isolation of membrane fractions kidneys were homogenized in isolation buffer and processed as described [2]. Total protein concentration was measured using the Pierce BCA Protein Assay reagent kit (Pierce, Schwerte, Germany) and controlled by Coomassie staining.

SDS-PAGE and Immunoblotting

Proteins were solubilized and SDS gel electrophoresis was performed on 8-10% polyacrylamide gels. After electrophoretic transfer of the proteins to nitrocellulose membranes, equity in protein loading and blotting was verified by membrane staining using 0.1% Ponceau red. Membranes were probed with primary antibodies and then exposed to HRP-conjugated secondary antibodies (Dianova, Hamburg, Germany). Immunoreactive bands were detected by chemiluminescence (Amersham Pharmacia, Glattbrugg, Switzerland). Densitometric evaluation was performed by BIO-PROFIL Bio-1D image software (Vilber Lourmat, Eberhardzell, Germany).

Immunohistochemistry

Cryosections were blocked with 5% skim milk/PBS, incubated with the respective primary antibody followed by the suitable cy-2 or cy-3-coupled secondary antibody (Dianova). Double-antibody staining procedure was controlled by parallel incubation of consecutive

sections, each probed only with one single antibody. Sections were analyzed using a multilaser confocal scanning microscope (SP5, Leica, Heerbrugg, Switzerland).

Antibodies

The following antibodies were used: rabbit anti-raptor (24C12), rabbit anti-rictor (53A2), rabbit anti-p70S6K (49D7), rabbit anti-phospho-p70S6K (108D2), rabbit anti-S6P (5G10), rabbit anti-phospho-S6P (D57.2.2E), rabbit anti-4E-BP1 (53H11), rabbit anti-p-4E-BP1 (T37/46, 236B4); all purchased from Cell Signaling Technologies and sheep anti-NDRG1, sheep anti-phospho-NDRG1 (kind gift of D. Alessi, University of Dundee, UK), guinea pig anti-megalin [3], goat anti-cubilin (Santa Cruz Biotechnology, Heidelberg, Germany, A-20),rabbit anti-clathrin (Abcam, Cambridge UK, ab 21679), rabbit- anti B^0AT1 [4], rabbit- anti y^+LAT1 [5], 4F2hc (CD98 M-20, Santa Cruz Biotechnology, Heidelberg, Germany), DOCK8 (ab121177 Abcam), BCL-x_L (54H6 Cell Signaling Technologies) and Alexa647-coubled phalloidin (ThermoFischer Scientific, Zug, Switzerland).

Electron microscopic evaluation

Ultrathin sections were analyzed using a transmission electron microscope Philips CM12. Images were taken from transverse sectioned S1 segments near the urinary pole and ultrastructural parameters such as microvilli length, number of microvilli per inner diameter length, number of total endocytic vesicles per cell area, number of early endosomes and late endosomes per cell area and mitochondria per cell area were evaluated morphometrically using Fiji software (1.49k). To avoid evaluation of tangentially sectioned epithelia, parallel alignment of BBM microvilli was used as a criterion. Only patent tubules were examined.

Cell culture, viral transfection and treatment

Opossum kidney cells (OKC) were kindly provided by H. Murer, University of Zürich, Switzerland. Cells were cultured at 37°C in 95% air/ 5% CO2 in high-glucose (450 mg/dl) DMEM supplemented with 5% fetal bovine serum, penicillin (100 U/ml), and streptomycin (100 µg/ml). OKC were transduced with recombinant adenovirus expressing shRNA targeting human p70S6K (S6K1) and rictor driven by the U6 promoter (kindly provided by Z. Yang, Fribourg, Switzerland [6]). Targeting sequences was in congruent with the respective opossum cDNA sequences. Viral titer was determined by QuickTiter™ Adenovirus Titer Immunoassay Kit (LuBio Science, Luzern, Switzerland). The control recombinant adenoviruses expressing shRNA targeting LacZ was from Invitrogen life Technologies, Zug, Switzerland. S6K1 targeting sequence: GGACATGGCAGGAGTGTTTGA; Rictor targeting sequence: ACTTGTGAAGAATCGTATCTT. At a confluence of 70-90% OKC were transduced with the recombinant adenovirus at titers of 100 MOI and cultured in complete medium for 3–5 days. Degree of knockdown was verified by TaqMan of S6K1 mRNA (Hs00177357_m1) compared to the housekeeping mRNA Tata-box binding protein (Mm00446973_m1) and the protein expression by western blot analysis of S6K1 and rictor. In comparison to MOCK transduction, OKC transduced with either S6K1 shRNA alone or S6K1 and rictor shRNA revealed a knockdown of S6K1 mRNA of -68 ± 12% and -67 ± 11%, $*p < 0.05$ respectively. S6K1 protein expression was reduced by -69 ± 15% and -63 ± 12%, respectively. Rictor protein expression was in comparison to MOCK transduction reduced by -66 ± 17% and by –87 ± 20% for OKC treated either with rictor shRNA alone or S6K1 and rictor shRNA, respectively.

In the case of endocytosis assay, cells were serum-starved overnight. Confluent OKC were incubated either for 3 days with various mTOR kinase inhibitors or overnight with various concentrations of rapamycin. Additionally, p70S6K specific inhibitor PF-4708671 incubated for 16-18h was used. If not otherwise indicated the following concentrations were used; 100 nM rapamycin, 250 nM torin, 100 nM PP242 and 3 µM and 10 µM PF-4708671 (Sigma

Aldrich) in FCS-free medium. 10 µM colchicine (Sigma Aldrich), a microtubule inhibitor, was always used overnight. Subsequently, the endocytosis assay was performed by incubating OKC with 0.1 mg/ml Alexa647-coupled albumin (Molecular Probes, Zug, Switzerland) for 30 minutes, followed by extensive washing, fixing with 3%PFA in PBS and flow cytometry measurements. The downstream effects of various concentrations of rapamycin incubated overnight was tested by immunoprecipitation of 4E-BP1 followed by western blot analysis of p-4E-BP1. Afterwards membranes were stripped and revealed with anti-4E-BP1 antibody. The ratios of p-4E-BP1/4E-BP1 with increasing concentrations of rapamycin were: 0 nM: 100 ± 31%, 5 nM: 79 ± 17%, 10 nM: 75 ± 7%, 100 nM 62 ± 13% and 500 nM: 63 ± 21 %.

Measurement of lysosomal pH and enzyme activity

The pH of lysosomes was measured with LysoSensor Yellow/Blue DND-160 (Molecular Probes, Zug, Switzerland) according to the manufacturer's protocol. In brief, OKC were collected by trypsin/EDTA and stained with LysoSensor at 1:200 concentrations in standard culture medium for 10 minutes followed by washing with PBS. Fluorescence of cell suspension in 2-(N-morpholino)ethanesulfonic acid (MES) buffer (pH 7.0) was measured by a microtiter plate at excitation 365 nm/emission 450 nm (for blue) and 485 nm/emission 550 nm (for yellow). Standard curves were obtained in each sample using pH-fixed MES-buffer (pH 4.0 - 6.5) with 10 µM nigericin (Sigma Aldrich, St. Gallen, Switzerland) and 10 µM monensin (Sigma Aldrich).

The activity of lysosomal enzymes was measured by incubating homogenate of virally transduced OK cells with the appropriate substrate. The reaction was allowed to proceed for 30 minutes at 37°C and then stopped with 5 mL of 85 mM glycine-carbonate buffer (pH 10.5). 200µL of homogenate was incubated with 100µL of 0.5 mM 4-methylumbelliferyl (MU)-β-galactoside in 100 mM citrate-phosphate buffer (pH 4.35) with 0.4 M NaCl. β-Glucuronidase was measured by incubating 200µL of homogenate with of 100µL of 1 mM 4-MU-β-d-glucuronide in 100 mM acetate buffer (pH 4.0). α-Mannosidase was measured by

incubating 50µL of homogenate with 100 µL of 4 mM 4-MU-α- d-mannopyranoside in 100 mM citrate-phosphate buffer (pH 4.0). The substrates were purchased from Sigma Aldrich, St. Gallen, Switzerland. The released 4-MU was measured against blank and standard 4-MU solutions. Fluorescence was determined with a Perkin Elmer 2030 Multilabel Reader Victor X3 at 450 nm after excitation at 360 nm.

D. melanogaster nephrocyte model system

D. melanogaster stocks were cultured on standard cornmeal molasses agar food and maintained at 25°C. RNAi-Based Nephrocyte Functional Screen Procedure: Virgins from MHC-ANF-RFP, HandGFP, and Dot-Gal4 transgenic lines (Gift from Zhe Han, University of Michigan, Ann Arbor, USA) were crossed to UAS-CG8487-RNAi (VDRC TID 42140/GD) males at 25°C; 2 days after crossing, flies were transferred to small collection cages with grape juice agar plates to collect the embryos for 24 hours at 25°C. Collected embryos were aged for 48 hours at 29° C and then subjected to examination of the RFP accumulation in pericardial nephrocytes using a confocal microscope. The RFP mean fluorescence intensity of GFP positive areas was measured to quantify the uptake efficiency.

Virgins of prospero-Gal4 (gift from Barry Denholm, University of Edinburgh, Edinburgh, UK) were crossed to UAS-CG8487-RNAi males (VDRC TID 42140/GD) for a GCN-specific knockdown of Gartenzwerg. GCN preparations for TEM were fixed in 4% PFA and 1 % Glutaraldehyde and embedded in low melting Agarose. Tissue samples were then embedded in epoxy resin (Durcopan, Plano, Germany). Ultrathin sections of 40nm thickness were analyzed using a Zeiss TEM 906 (Zeiss, Oberkochen, Germany).

Sample preparation for MS/MS

Snap frozen kidney cortex were homogenized on ice and solubilized in 8M cold urea buffer containing 50mM ammonium bicarbonate and 1x Protease and phosphatase inhibitor cocktail (Pierce, ThermoFischer Scientific, Rockford, USA). Lysates were cleared with a 20 min spin of 20.000 g in a benchtop centrifuge. Next, the supernatant was recovered and proteins were reduced, alkylated and digested at a 1:100 w/w trypsin/total protein ratio as previously described [7]. Protein abundance was measured using a commercial BCA assay (Pierce). 5% of the digest was retained for proteomic analysis. 800 µg of the remaining peptides was subjected to phosphopeptide enrichment using Fe-NTA immobilized metal affinity chromatography columns (Pierce) without further fractionation as previously described [7, 8]. All samples were cleaned up using C18 resin in stage tips as previously described [9].

Nano-liquid chromatography and mass spectrometry

The cleaned peptides were separated using nLC on a house-packed 50cm C18 column in a column oven. The particle size was 1.7 µm C18 beads (Dr Maisch GmbH, Ammerbuch-Entringen, Germany). We analyzed the peptides using the following solvent gradient with ascending concentrations of buffer B as compared to buffer A.: t=0min; 4% [Buffer B], 05 min, 6%; 125 min, 23%; 132 min, 54%; 138 min, 85% ; 143 min, 85%; 145 min 5%). Buffer B was 80% ACN, 0.1% FA and buffer A was 0.1% FA. The flow rate was constant with 250 nl/min. The phosphopeptides were separated using nLC with the following gradient (0min, 10% [Buffer B]; 5min, 10%; 125 min; 38%, 132 min 60%; 138, 95; 143, 95%; 148 min; 95% and 148 min 5%) Peptides were directly sprayed into a quadrupole-orbitrap based mass spectrometer QExactive Plus (Thermo) run in positive ion mode as previously described [10]. The acquisition parameters were as follows: A MS1 precursor scan was followed by 10 MS2 scans of the most intense ions (Top10 method). The resolution was 70000 for MS1 scans and 17500 for MS2 scans. AGC target was 3e6 for MS1 scans, and 5e5 for MS2 scans.

Mass range was 300-1750 m/z for MS1 scans, and 200-2000 m/z for MS2 scans. Isolation window was 2.1 m/z, dynamic exclusion was enabled (20s).

Bioinformatic analysis

Raw files were searched using the MaxQuant software package, v 1.5.1.0 [11], including LFQ algorithm [12]. The raw data were searched against a recent uniprot reference proteome database for mouse including common potential contaminants (Decoy mode: revert). The parameters were mainly default with a few modifications: Carbamidomethylation of cysteins as fixed modification, deisotoping enabled, mass accuracy for first search 20ppm, for second search 4.5 ppm. PSM, protein and site FDR was set to 0.01, minimal peptide length was 7, score for unmodified peptides was 0, and modified was 16. At least one peptide was necessary for protein identification. Variable modifications included N-terminal acetylation and methionine oxidation. In addition, phosphorylation (mass shift approximately +80) on STY residue was added as a variable modification for samples enriched for phosphorylated peptides. Match between runs (matching time 0.7min, matching window 20min) and label free quantification was enabled. At least 2 counts were necessary for a ratio. The MaxQuant output .txt files (PhosphoSTY.txt and proteingroups.txt) were then analyzed, visualized and normalized using the Perseus software, v. 1.5.1.0. For LFQ, only 5 missing values were tolerated, and for phosphorylation sites no missing value was tolerated. All other proteins or sites were filtered from the dataset. Two samples, for which identification count and/or MS/MS run was not sufficient (protein identification number less than -1SD from the mean) were removed entirely from the analysis. Missing values were imputed (SD downshift 1.8, width 0.3) after logarithmizing intensities and checking for normal distribution. Hierarchical clustering was performed based on the Euclidean distance. Vulcano plots were generated after a paired two-sample t-test. To determine significantly changed proteins, and to circumvent the multiple testing problem, a statistical approach similar to significance analysis of microarrays (SAM) [13] was utilized. This approach can also be applied to proteomics data. The threshold for significance was 0.3 after 250 randomizations (s0=1). Proteins and

phosphorylation sites considered significant were exported and depicted in the respective tables. GO terms, keywords (uniprot) as well as PFAM domains and KEGG pathways were annotated using the Perseus annotation packages. Next, a fishers exact test was performed to assess whether there were special categories overrepresented in the changed protein and site populations as compared to the non-changed entities (for proteins, this test was performed separately for the significantly increased and the significantly decreased proteins). The significantly changed GO terms were reanalyzed and condensed using Revigo [14] and visualized in Cytoscape [15]. The cumulative histogram was generated using the Prism (Graphpad) software. Phosphorylation motifs of the upregulated or downregulated phosphopeptide population were generated using the phosphologo software [16]. Known phosphosites, known substrates and regulatory sites were added manually to the Table S4. Using a binary decision tree we separated the phosphorylation motifs in “basophilic”, “proline-directed”, “acidophilic” and “others”. [17]

All MS raw files, including search results and metadata, are deposited at the ProteomeXchange repository [18]. **Project accession:** PXD002422 (http://www.ebi.ac.uk/pride/archive/projects/PXD002422).

Supplemental Figure Legends

Supplementary Fig. 1. Triple labeling of either mTOR, RAPTOR, S6K1, S6P or NDRG1 (red); megalin (green) and phalloidin to stain actin filaments (blue) on control mouse renal sections. (A) mTOR is localized to the subapical membrane region, (A') merged image demonstrating proximal tubular expression. Insert of (A') is depicted in (A'') showing mTOR localized in vicinity to megalin. (B) RAPTOR localizes to vesicles of the subapical membrane region of S1 and S2 portions of the proximal tubule, (B′) merged image demonstrating proximal tubular expression. For more detailed analysis insert of (B′) is depicted in (B′′) presenting a partial overlap between RAPTOR and megalin. (C) S6K1 is found in vesicular structures of the subapical membrane region and throughout the cytoplasm, (C') merged image demonstrating proximal tubular expression. Note, S3 segments marked by an asterisk are devoid of vesicular expression and show only intracellular staining. Insert of (C′) is depicted in (C′′) showing the vesicular structures positive for S6K1 and megalin in the S1 segment. (D) Ribosomal S6 protein (S6P) is found in the apical membrane region of the proximal tubule; (D′) merged image is verifying proximal tubular expression. Insert of (D′) is depicted in (D′′) showing ribosomal S6P expression in close vicinity to megalin with occasional overlap. (E) NDRG1 is found to be expressed in the apical membrane region of the convoluted part of the proximal tubule; (E') merged image is verifying proximal tubular expression. Asterisk marks the S3 segment of the proximal tubule which lacks a NDRG1 signal. Insert of (E') is depicted in (E'') showing partial coexpression of NDRG1 and megalin. Magnification as indicated by scale bar.

Supplementary Fig. 2. (A) Urinary acidic and basic amino acid excretion of $Rap^{\Delta Tubule}$, $Ric^{\Delta Tubule}$ and $RapRic^{\Delta Tubule}$. (B) Serum concentration of neutral, acidic and basic amino acids of $Rap^{\Delta Tubule}$, $Ric^{\Delta Tubule}$ and $RapRic^{\Delta Tubule}$. **P*-value vs. control <0.05; ** *P*-value vs. control <0.01.

Supplementary Fig.3. Immunohistochemical staining of MEGALIN (A) and CUBILIN (B) on $Rap^{\Delta Tubule}$, $Ric^{\Delta Tubule}$ and $RapRic^{\Delta Tubule}$ in comparison to their respective control. (C) Western blot analysis of MEGALIN from $Rap^{\Delta Tubule}$, $Ric^{\Delta Tubule}$ and $RapRic^{\Delta Tubule}$. Densitometric analysis of MEGALIN western blots from $Rap^{\Delta Tubule}$, $Ric^{\Delta Tubule}$ and $RapRic^{\Delta Tubule}$. No significant difference in expression intensity or subcellular distribution were observed.

Supplementary Fig. 4. Histological alterations of $Rap^{\Delta Tubule}$ and $RapRic^{\Delta Tubule}$ 3 month after induction. (A) PAS-stained paraffin sections of Con, $Rap^{\Delta Tubule}$ and $RapRic^{\Delta Tubule}$. Black stippled line indicates boundary between cortex and outer medulla and yellow stippled line boundary between outer stripe and inner stripe. (B) Expression of MEGALIN from Con, $Rap^{\Delta Tubule}$ and $RapRic^{\Delta Tubule}$. (C) Expression of CUBILIN from Con, $Rap^{\Delta Tubule}$ and $RapRic^{\Delta Tubule}$. (D) Expression of Na^+/K^+-ATPase (NKA) from Con, $Rap^{\Delta Tubule}$ and $RapRic^{\Delta Tubule}$. Distal tubules are indicated by an asterisk. Missorting of NKA containing vesicles towards the apical membrane in $Rap^{\Delta Tubule}$ and $RapRic^{\Delta Tubule}$ and reduced basolateral expression in $RapRic^{\Delta Tubule}$ is shown. Magnification as indicated by scale bar.

Supplementary Fig. 5. Pharmacological inhibition of mTORC1, mTORC1/2 or P70S6K1 and knock-down of mTORC2 and/or P70S6K1-induced signaling in proximal tubule cells. (A) Quantitative evaluation of flow cytometrical analysis of endocytosis assay performed in opossum kidney cells (OKC) treated for 3 days with 100 nM rapamycin, 100 nM PP242 and 250 nM torin or overnight with 10 µM colchicine. Representative image of flow cytometrical analysis (right). (B) Quantitative evaluation of flow cytometrical analysis of endocytosis assay performed on OKC treated with increasing concentrations of rapamycin or colchicine overnight. Representative image of flow cytometrical analysis (right). (C) Quantitative evaluation of flow cytometrical analysis of endocytosis assay performed on OKC treated with 3µM and 10 µM PF-4708671 (PF) and 100nM rapamycin for 16-18 hours. Representative image of flow cytometrical analysis (right). (D) Quantitative evaluation of flow

cytometrical analysis of endocytosis assay performed on viral transduced OKC with knockdown of S6K1, RICTOR or both proteins. Representative image of flow cytometrical analysis (right). (E) Lysosomal pH of virally transduced OKC with knockdown of S6K1, RICTOR or both proteins. (F) Quantitative assessment of clathrin-coated vesicles per μm^3 of virally transduced OKC with knockdown of S6K1, RICTOR or both proteins. (G) Representative images of merged z-scans in a 3D illustration are depicted. Scale bar = 40 μm. **P*-value vs. control <0.05; ** *P*-value vs. control <0.01; $^{\#}$*P*-value vs. control <0.001.

Supplemental tables

Supplemental Table 1. Physiological parameters of Con, Rap$^{\Delta Tubule}$, Ric$^{\Delta Tubule}$ and RapRic$^{\Delta Tubule}$. All values are rounded means given with min-max and n-number. *P-value vs. control <0.05; ** P-value vs. control <0.01.

Supplemental Table 2. Quantitative electron microscopy analysis. Microvilli length, number of microvilli per length cell surface, number of vesicles per cell area and mitochondrial area per cell area given in % of Rap$^{\Delta Tubule}$, Ric$^{\Delta Tubule}$ and RapRic$^{\Delta Tubule}$ in comparison to their respective controls. *P-value vs. control <0.05; **P-value vs. control <0.01; $^{\#}P$-value vs control <0.001.

Supplemental Table 3. Identified proteins with significant changes in expression level of Rap$^{\Delta Tubule}$ in comparison to control. (A) Proteins which were significantly increased, (B) proteins which were significantly reduced.

Supplemental Table 4. Identified changes of phosphorylation level of proteins of Rap$^{\Delta Tubule}$ in comparison to control. (A) Phosphorylation sites of proteins which were significantly increased, (B) phosphorylation sites of proteins which were significantly reduced. In addition known phosphosites, substrates and regulatory sites are indicated.

Supplemental Information References

1. Schell, C, Baumhakl, L, Salou, S, Conzelmann, AC, Meyer, C, Helmstadter, M, Wrede, C, Grahammer, F, Eimer, S, Kerjaschki, D, Walz, G, Snapper, S, Huber, TB: N-wasp is required for stabilization of podocyte foot processes. *Journal of the American Society of Nephrology : JASN,* 24**:** 713-721, 2013.
2. Gadau, J, Peters, H, Kastner, C, Kuhn, H, Nieminen-Kelha, M, Khadzhynov, D, Kramer, S, Castrop, H, Bachmann, S, Theilig, F: Mechanisms of tubular volume retention in immune-mediated glomerulonephritis. *Kidney International,* 75**:** 699-710, 2009.
3. Theilig, F, Kriz, W, Jerichow, T, Schrade, P, Hahnel, B, Willnow, T, Le Hir, M, Bachmann, S: Abrogation of protein uptake through megalin-deficient proximal tubules does not safeguard against tubulointerstitial injury. *Journal of the American Society of Nephrology : JASN,* 18**:** 1824-1834, 2007.
4. Romeo, E, Dave, MH, Bacic, D, Ristic, Z, Camargo, SM, Loffing, J, Wagner, CA, Verrey, F: Luminal kidney and intestine SLC6 amino acid transporters of B0AT-cluster and their tissue distribution in Mus musculus. *American Journal of Physiology - Renal physiology,* 290**:** F376-383, 2006.
5. Dave, MH, Schulz, N, Zecevic, M, Wagner, CA, Verrey, F: Expression of heteromeric amino acid transporters along the murine intestine. *The Journal of Physiology,* 558**:** 597-610, 2004.
6. Xiong, Y, Yepuri, G, Forbiteh, M, Yu, Y, Montani, JP, Yang, Z, Ming, XF: ARG2 impairs endothelial autophagy through regulation of MTOR and PRKAA/AMPK signaling in advanced atherosclerosis. *Autophagy,* 10**:** 2223-2238, 2014.

7. Rinschen, MM, Wu, X, Konig, T, Pisitkun, T, Hagmann, H, Pahmeyer, C, Lamkemeyer, T, Kohli, P, Schnell, N, Schermer, B, Dryer, S, Brooks, BR, Beltrao, P, Krueger, M, Brinkkoetter, PT, Benzing, T: Phosphoproteomic analysis reveals regulatory mechanisms at the kidney filtration barrier. *JASN,* 25**:** 1509-1522, 2014.

8. Rinschen, MM, Yu, MJ, Wang, G, Boja, ES, Hoffert, JD, Pisitkun, T, Knepper, MA: Quantitative phosphoproteomic analysis reveals vasopressin V2-receptor-dependent signaling pathways in renal collecting duct cells. *PNAS,* 107**:** 3882-3887, 2010.

9. Rappsilber, J, Ishihama, Y, Mann, M: Stop and go extraction tips for matrix-assisted laser desorption/ionization, nanoelectrospray, and LC/MS sample pretreatment in proteomics. *Analytical Chemistry,* 75**:** 663-670, 2003.

10. Nolte, H, Konzer, A, Ruhs, A, Jungblut, B, Braun, T, Kruger, M: Global protein expression profiling of zebrafish organs based on in vivo incorporation of stable isotopes. *Journal of Proteome Research,* 13**:** 2162-2174, 2014.

11. Cox, J, Mann, M: MaxQuant enables high peptide identification rates, individualized p.p.b.-range mass accuracies and proteome-wide protein quantification. *Nature Biotechnology,* 26**:** 1367-1372, 2008.

12. Cox, J, Hein, MY, Luber, CA, Paron, I, Nagaraj, N, Mann, M: Accurate proteome-wide label-free quantification by delayed normalization and maximal peptide ratio extraction, termed MaxLFQ. *Molecular & Cellular Proteomics : MCP,* 13**:** 2513-2526, 2014.

13. Tusher, VG, Tibshirani, R, Chu, G: Significance analysis of microarrays applied to the ionizing radiation response. *PNAS,* 98**:** 5116-5121, 2001.

14. Supek, F, Bosnjak, M, Skunca, N, Smuc, T: REVIGO summarizes and visualizes long lists of gene ontology terms. *PloS One,* 6**:** e21800, 2011.

15. Shannon, P, Markiel, A, Ozier, O, Baliga, NS, Wang, JT, Ramage, D, Amin, N, Schwikowski, B, Ideker, T: Cytoscape: a software environment for integrated models of biomolecular interaction networks. *Genome Research,* 13**:** 2498-2504, 2003.

16. Douglass, J, Gunaratne, R, Bradford, D, Saeed, F, Hoffert, JD, Steinbach, PJ, Knepper, MA, Pisitkun, T: Identifying protein kinase target preferences using mass spectrometry. *American Journal of Physiology Cell Physiology,* 303**:** C715-727, 2012.

17. Villen, J, Beausoleil, SA, Gerber, SA, Gygi, SP: Large-scale phosphorylation analysis of mouse liver. *PNAS,* 104**:** 1488-1493, 2007.

18. Vizcaino, JA, Deutsch, EW, Wang, R, Csordas, A, Reisinger, F, Rios, D, Dianes, JA, Sun, Z, Farrah, T, Bandeira, N, Binz, PA, Xenarios, I, Eisenacher, M, Mayer, G, Gatto, L, Campos, A, Chalkley, RJ, Kraus, HJ, Albar, JP, Martinez-Bartolome, S, Apweiler, R, Omenn, GS, Martens, L, Jones, AR, Hermjakob, H: ProteomeXchange provides globally coordinated proteomics data submission and dissemination. *Nature Biotechnology,* 32**:** 223-226, 2014.

Supplemental Figure 1

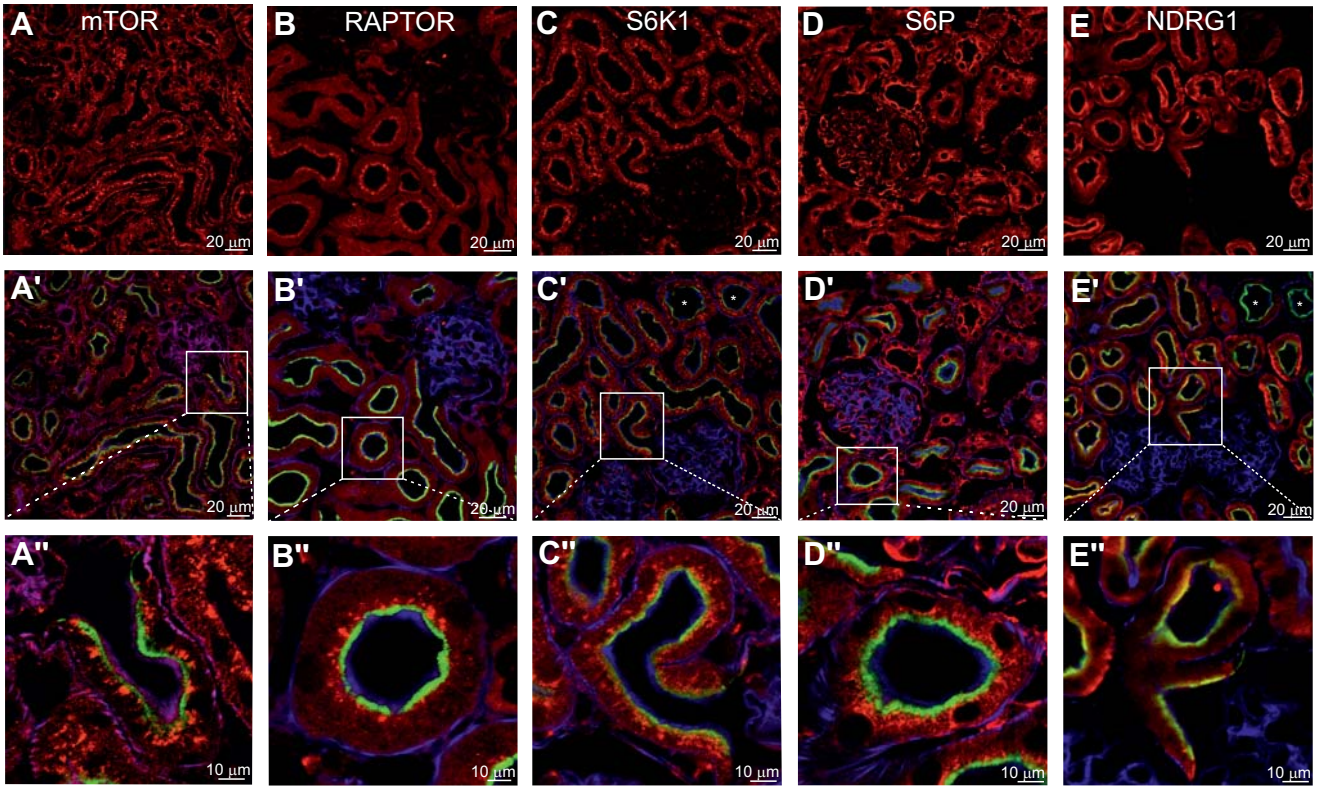

Supplemental Figure 2

A

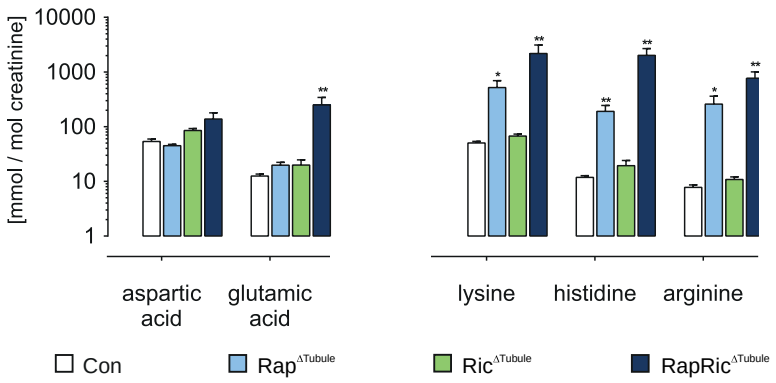

B

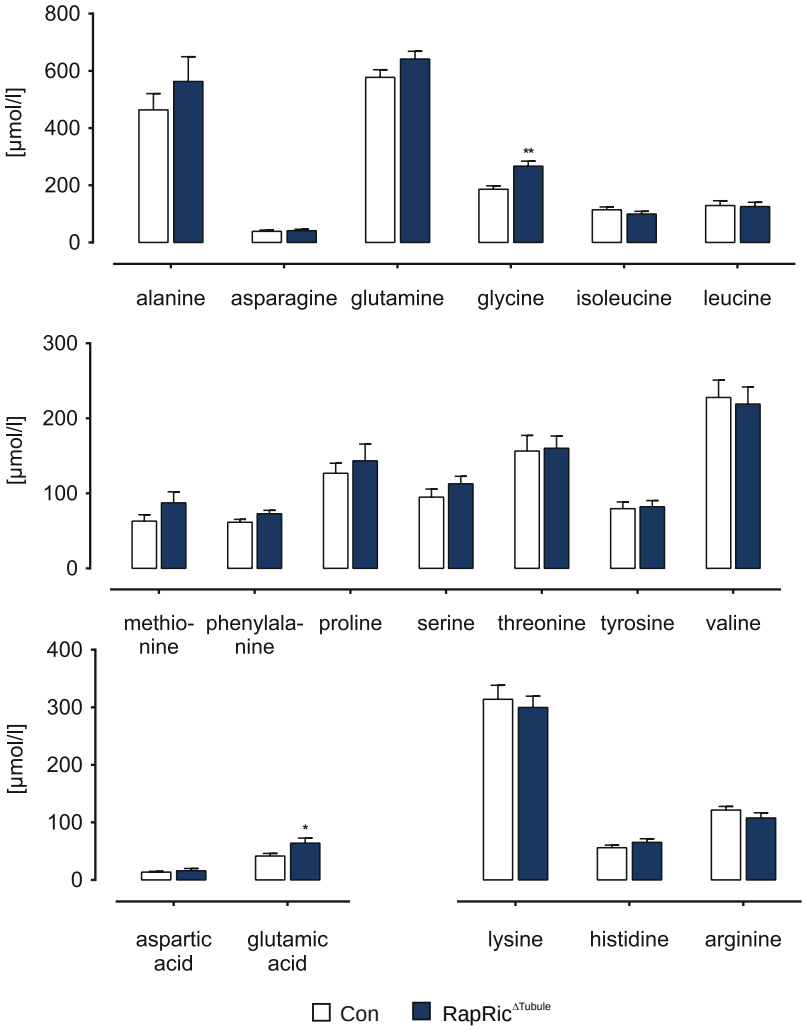

Supplemental Figure 3

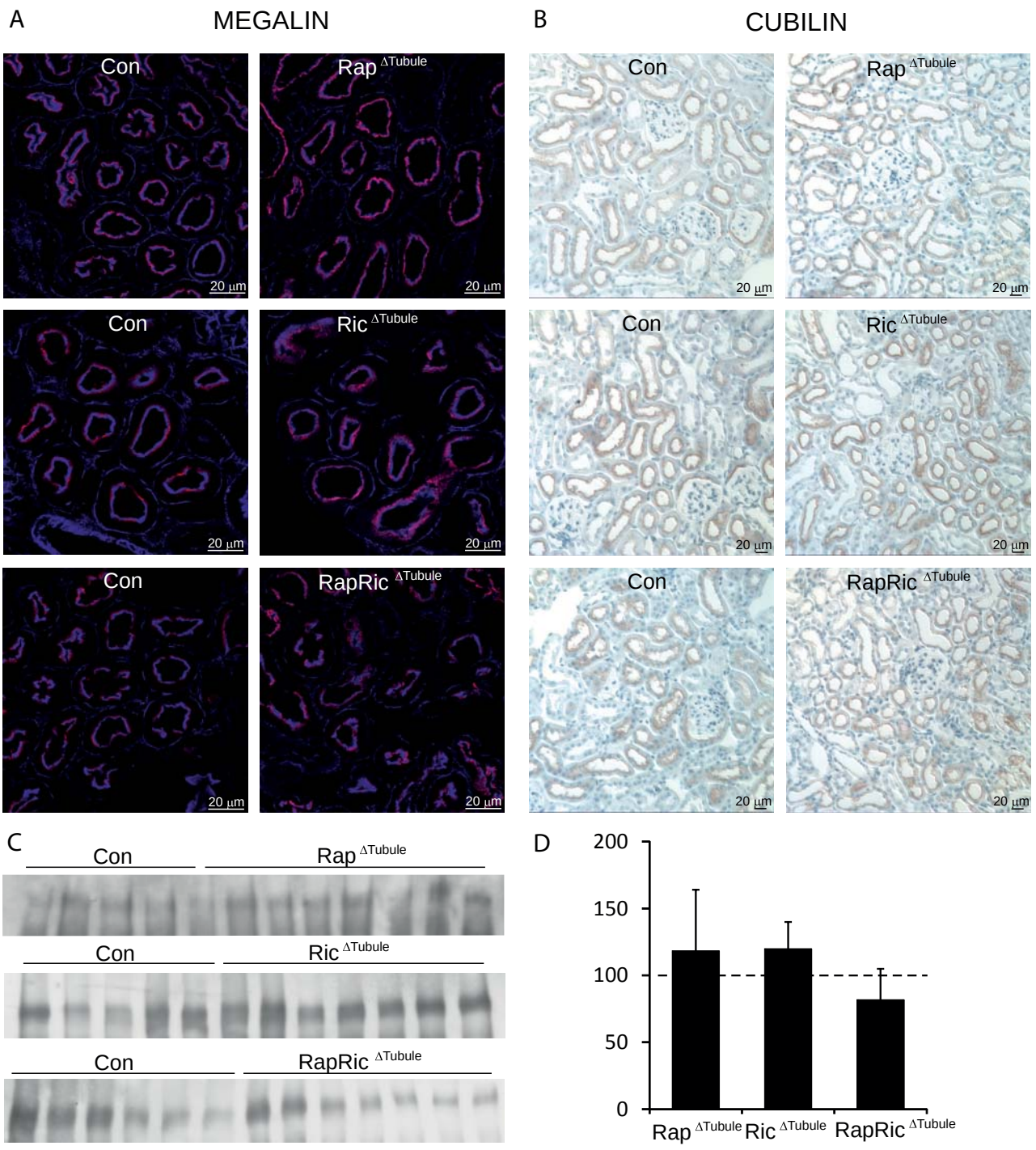

Supplemental Figure 4

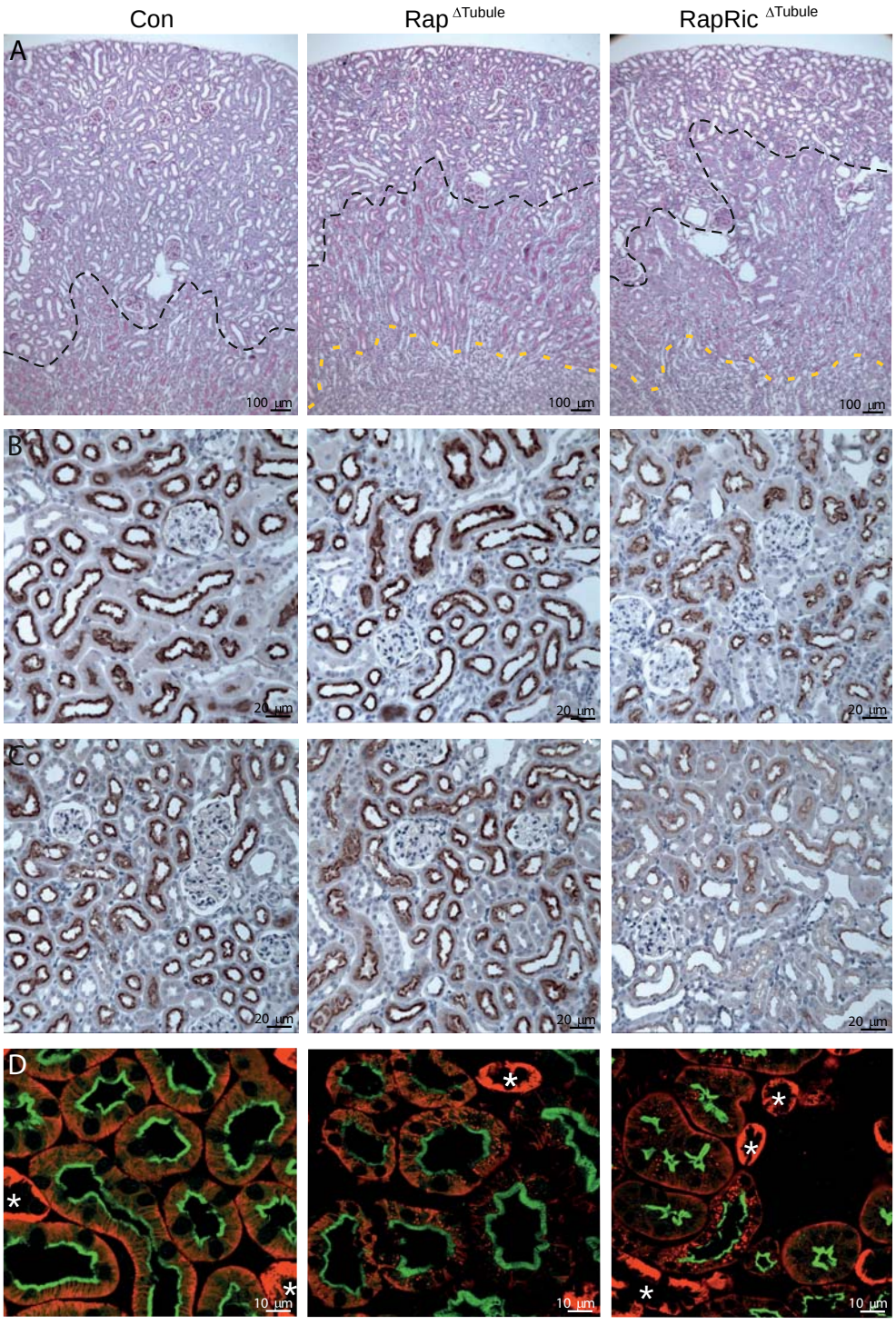

Supplemental Figure 5

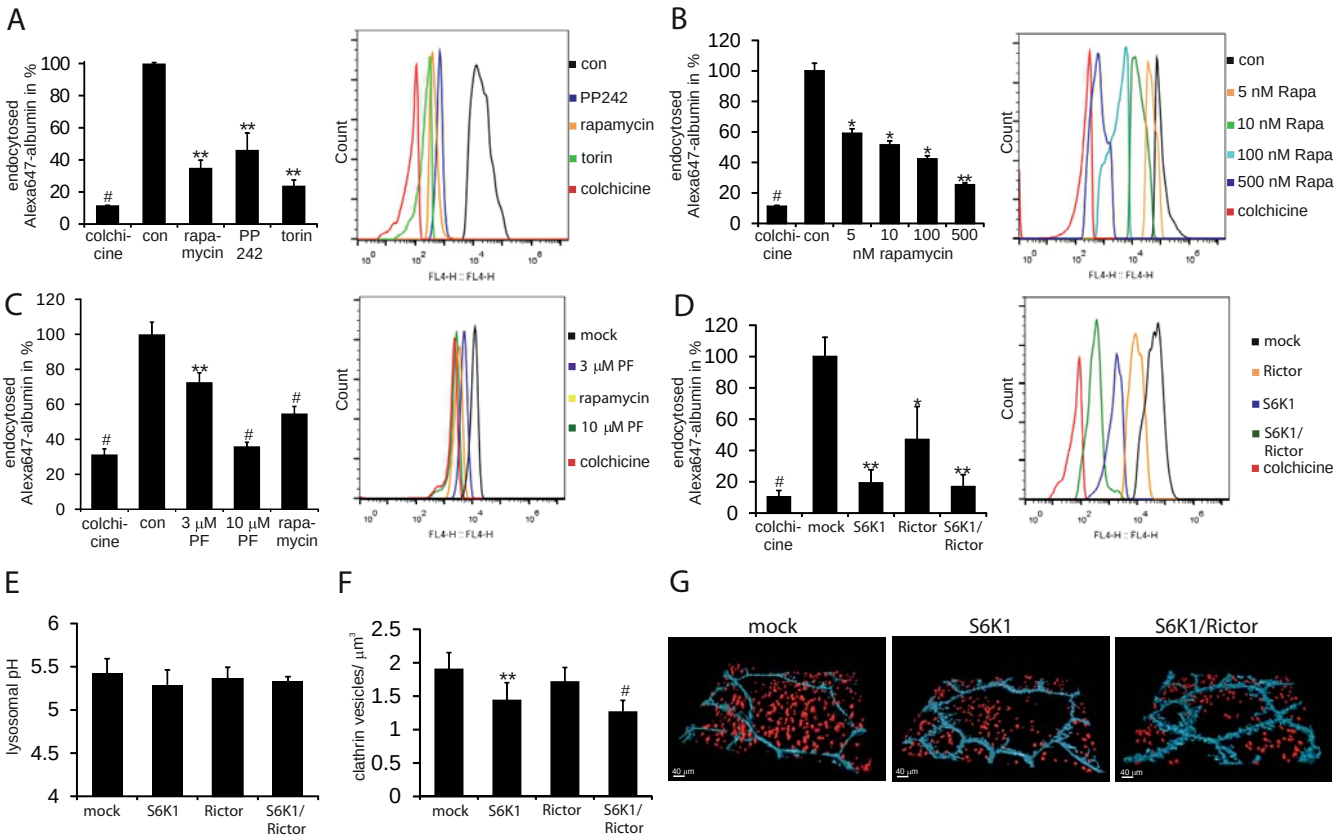

	Con	Rap$^{\Delta Tubule-}$	Ric$^{\Delta Tubule}$	RapRic$^{\Delta Tubule}$
body weight (g)	28,9 [27,5-30,3], (n=50)	27,7 [25,9-29,5], (n=19)	25,2 [23,1-27,2], (n=12)	24,0 [22,3-25,7] **, (n=19)
food intake (mg/ g body weight)	99 [91-108], (n=42)	118 [102-134] *, (n=12)	109 [98-120], (n=12)	127 [111-143] **, (n=15)
fluid intake (µl/ g body weight)	218 [166-270], (n=39)	675 [458-892] **, (n=12)	233 [135-331], (n=11)	407 [329-484] **, (n=15)
serum urea (mg/dl)	53 [42-64], (n=17)	62 [47-78], (n=6)	61 [40-81], (n=6)	105 [84-126] **, (n=6)
urine volume (µl/ g body weight)	50 [39-60], (n=42)	387 [206-568] **, (n=12)	58 [29-87], (n=12)	140 [109-172] *, (n=15)
urinary sodium (µmol/ mg crea/ g food)	148 [134-162], (n=41)	195 [127-263] *, (n=12)	152 [115-190], (n=12)	208 [173-243] **, (n=15)
urinary potassium (µmol/ mg crea/ g food)	241 [216-162], (n=41)	291 [211-370], (n=12)	211 [196-225], (n=12)	315 [262-368], (n=15)
urinary calcium (µmol/ mg crea/ g food)	1,5 [1,1-1,8], (n=38)	2,5 [1,4-3,6], (n=12)	1,0 [0,7-1,4], (n=12)	1,9 [1,4-2,4], (n=15)

Table 1 - Physiologic parameter
Values are rounded means + 95%CI, * = p-value vs Con < 0,05, ** = p-value vs Con < 0,01

Table 2

	microvilli lenght in µm	number of microvilli per µm lenght cell surface	Number of vesicles per cell area	Mitochondria in %
Con	1.71 ± 0.23	4.91 ± 0.41	1.01 ± 0.14	40.53 ± 5.13
$Rap^{\Delta Tubule}$	1.25 ± 0.04**	3.42 ± 0.49$^{\#}$	0.71 ± 0.04**	37.42 ± 2.35
Con	1.52 ± 0.19	5.05 ± 0.61	1.05 ± 0.12	41.45 ± 5.77
$Ric^{\Delta Tubulue}$	1.31 ± 0.17*	3.38 ± 0.65*	0.83 ± 0.15*	37.52 ± 3.57
Con	1.55 ± 0.16	4.81 ± 0.44	1.00 ± 0.12	39.58 ± 2.71
$RapRic^{\Delta Tubule}$	1.06 ± 0.05$^{\#}$	2.98 ± 0.17$^{\#}$	0.58 ± 0.06$^{\#}$	32.12 ± 3.47*

A. Proteins increased in Rap $^{\Delta Tubule}$ as compared to control

Gene names	Uniprot	Protein names	log_2 intensity (Rap/control)	-log(P-value)
Obp1a	Q9D3H2	MCG117626	3,02	2,50
Rplp1	P47955	60S acidic ribosomal protein P1	2,93	1,49
Ipo4	Q8VI75	Importin-4	2,65	1,58
Reg3g	O09049	Regenerating islet-derived protein 3-gamma	2,64	1,47
Parpbp	Q6IRT3	PCNA-interacting partner	2,62	0,67
Ppp2r4	P58389	Serine/threonine-protein phosphatase 2A activator	2,55	2,64
Retn	Q99P87	Resistin	2,54	3,80
Ahsg	P29699	Alpha-2-HS-glycoprotein	2,51	3,55
Gm14743	A2BHD2	Protein Gm14743	2,38	2,78
Reg1	P43137	Lithostathine-1	2,33	2,12
Guca2b	O09051	Guanylate cyclase activator 2B	2,26	4,00
Ambp	Q07456	Protein AMBP	2,24	3,56
Napsa	O09043	Napsin-A	2,23	1,75
Cops7a	Q9CZ04	COP9 signalosome complex subunit 7a	2,20	1,93
Scgb1a1	Q06318	Uteroglobin	2,16	1,42
Apoa4	P06728	Apolipoprotein A-IV	2,11	3,39
Ttr	P07309	Transthyretin	2,10	2,25
Agt	P11859	Angiotensinogen	2,04	3,98
Serpinf1	P97298	Pigment epithelium-derived factor	2,03	3,12
Gm2a	Q60648	Ganglioside GM2 activator	2,00	4,89
Lyz2	P08905	Lysozyme C-2	1,99	4,12
Rbp4	Q00724	Retinol-binding protein 4	1,93	2,00
S100a6	P14069	Protein S100-A6	1,90	1,24
Apoc3	P33622	Apolipoprotein C-III	1,89	2,41
Cst3	P21460	Cystatin-C	1,87	4,07
Rnase4	Q8C7E4	Ribonuclease 4	1,87	3,36
Cpq	Q9WVJ3	Carboxypeptidase Q	1,86	1,37
Gc	P21614	Vitamin D-binding protein	1,82	3,40
Cox6b1	P56391	Cytochrome c oxidase subunit 6B1	1,75	1,17
Ctbs	Q8R242	Di-N-acetylchitobiase	1,74	2,73
Chi3l3	O35744	Chitinase-3-like protein 3	1,66	3,28
Slc37a4	Q9D1F9	Protein Slc37a4	1,63	0,83
Chchd2	Q9D1L0	Coiled-coil-helix-coiled-coil-helix domain-containing protein 2, mitochondrial	1,62	1,68
Nup155	Q99P88	Nuclear pore complex protein Nup155	1,59	1,39
Dsg4	Q7TMD7	Desmoglein-4	1,55	0,70
Igfbp2	D3YU40	Insulin-like growth factor-binding protein 2	1,55	1,50
C4b	P01029	Complement C4-B	1,54	3,38
Arl2	Q9D0J4	ADP-ribosylation factor-like protein 2	1,54	2,18
Tgfb1i1	E9PYQ1	Transforming growth factor beta-1-induced transcript 1 protein	1,54	1,76
Cd5l	Q9QWK4	CD5 antigen-like	1,52	4,55
Cfb	P04186	Complement factor B	1,52	1,68
Kng2	Q6S9I0	Kng2 protein	1,49	1,82
Eva1a	D3Z511	Protein eva-1 homolog A	1,48	2,18
N/A	P01837	Ig kappa chain C region	1,47	1,99
S100a10	P08207	Protein S100-A10	1,47	1,47
Snrpb	P27048	Small nuclear ribonucleoprotein-associated protein B	1,46	1,18
Abhd11	Q8K4F5	Alpha/beta hydrolase domain-containing protein 11	1,44	0,84
Sept6	Q9R1T4	Septin-6	1,44	1,70
Prelp	Q9JK53	Prolargin	1,43	1,47
Mtx2	O88441	Metaxin-2	1,42	0,90
Ctbp1	O88712	C-terminal-binding protein 1	1,40	0,71
Retnlg	Q8K426	Myeloid cysteine-rich protein	1,39	1,59
Lsm14a	Q8K2F8	Protein LSM14 homolog A	1,39	1,32
Cyp4a12a	Q91WL5	Cytochrome P450 4A12A	1,37	0,76
Nek7	Q9ES74	Serine/threonine-protein kinase Nek7	1,37	1,59
Uqcrq	Q9CQ69	Cytochrome b-c1 complex subunit 8	1,36	0,78
Amy1	P00687	Alpha-amylase 1	1,36	0,83
Hao2	Q9NYQ2	Hydroxyacid oxidase 2	1,34	2,07
Glyctk	Q8QZY2	Glycerate kinase	1,33	1,77
Snrnp40	Q6PE01	U5 small nuclear ribonucleoprotein 40 kDa protein	1,32	1,09
Hpx	Q91X72	Hemopexin	1,29	2,53
Tstd1	E9PY03	Protein Tstd1	1,26	1,09
Slc10a2	P70172	Ileal sodium/bile acid cotransporter	1,24	1,97
B2m	P01887	Beta-2-microglobulin	1,23	2,45
Erp29	P57759	Endoplasmic reticulum resident protein 29	1,22	1,45

Apoa1	Q00623	Apolipoprotein A-I	1,21	1,92
Spink3	P09036	Serine protease inhibitor Kazal-type 3	1,19	2,68
Snrpc	Q62241	U1 small nuclear ribonucleoprotein C	1,19	0,97
Myg1	F8WGG3	UPF0160 protein MYG1, mitochondrial	1,16	1,93
Hamp	Q9EQ21	Hepcidin	1,16	1,78
Nt5e	Q61503	5-nucleotidase	1,13	1,63
Them7	Q9DCP4	Novel Thioesterase superfamily domain and Saposin A-type domain contain	1,13	3,68
Eefsec	Q9JHW4	Selenocysteine-specific elongation factor	1,12	1,57
Man2b1	O09159	Lysosomal alpha-mannosidase	1,12	1,55
Fnbp1l	E9PUK3	Formin-binding protein 1-like	1,11	1,34
N/A	P01843	Ig lambda-1 chain C region	1,11	1,49
Tpm1	B7ZNL3	ropomyosin alpha-1 chain	1,09	1,62
Enpep	P16406	Glutamyl aminopeptidase	1,04	2,18
Ace2	Q8R0I0	Angiotensin-converting enzyme 2	1,04	3,46
Blvrb	Q923D2	Flavin reductase (NADPH)	1,02	2,18
Ren1	P06281	Renin-1	1,01	2,01
Fdx1l	Q9CPW2	Adrenodoxin-like protein, mitochondrial	0,98	1,53
Cpsf6	Q6NVF9	Cleavage and polyadenylation specificity factor subunit 6	0,97	1,63

B. Proteins decreased in Rap $^{\Delta Tubule}$ as compared to control

Gene names	Uniprot	Protein names	log_2 intensity (Rap/control)	-log(P-value)
Thsd4	Q3UTY6	Thrombospondin type-1 domain-containing protein 4	-2,79	0,98
4933436I01F	Q9D3T1	Protein 4933436I01Rik	-2,73	1,18
Dock8	Q8C147	Dedicator of cytokinesis protein 8	-2,70	0,82
Dnah10	F7ABZ6	Protein Dnah10	-2,50	1,89
Slc26a1	P58735	Sulfate anion transporter 1	-2,22	1,30
Slc7a7	Q9Z1K8	Y+L amino acid transporter 1	-2,08	1,55
Bloc1s5	Q8R015	Biogenesis of lysosome-related organelles complex 1 subunit 5	-1,89	0,64
Rtn3	Q9ES97	Reticulon-3	-1,89	1,17
Ppp6r1	Q7TSI3	Serine/threonine-protein phosphatase 6 regulatory subunit 1	-1,73	2,61
Dnajc12	Q9R022	DnaJ homolog subfamily C member 12	-1,57	3,45
Bcl2l1	A2AHX9	Bcl-2-like protein 1	-1,55	1,03
Fbxo22	D6REV6	F-box only protein 22	-1,55	2,20
Slc6a19	D6RJ80	Sodium-dependent neutral amino acid transporter B(0)AT1	-1,54	1,22
Slc5a12	Q49B93	Sodium-coupled monocarboxylate transporter 2	-1,51	4,94
Rab10	P61027	Ras-related protein Rab-10	-1,48	1,25
Uros	Q3TPL3	Uroporphyrinogen-III synthase	-1,44	0,82
Cbx1	P83917	Chromobox protein homolog 1	-1,39	0,95
Sdc4	O35988	Syndecan-4	-1,39	1,39
Cyp51a1	Q8K0C4	Lanosterol 14-alpha demethylase	-1,38	1,20
Ankrd44	J3QK13	Serine/threonine-protein phosphatase 6 regulatory ankyrin repeat subunit B	-1,35	0,94
Snx8	Q8CFD4	Sorting nexin-8	-1,24	1,05
Phgdh	Q61753	D-3-phosphoglycerate dehydrogenase	-1,21	3,57
Mrpl13	Q9D1P0	39S ribosomal protein L13, mitochondrial	-1,20	1,26
Larp1	Z4YJT3	La-related protein 1	-1,13	1,68
Nccrp1	G3X9C2	F-box only protein 50	-1,12	1,06
G6pc	P35576	Glucose-6-phosphatase	-1,11	1,04
Slc16a1	P53986	Monocarboxylate transporter 1	-1,10	3,58
Hspa14	Q99M31	Heat shock 70 kDa protein 14	-1,09	1,22
Glul	P15105	Glutamine synthetase	-1,08	4,29
Chd4	E9QAS4	Chromodomain-helicase-DNA-binding protein 4	-1,02	1,47
Rhot1	Q8BG51	Mitochondrial Rho GTPase 1	-1,00	1,45
Slc43a2	Q8CGA3	Large neutral amino acids transporter small subunit 4	-1,00	2,96
Rpl6	P47911	60S ribosomal protein L6	-0,99	2,74
Rpl7	P14148	60S ribosomal protein L7	-0,93	1,79
Rpl26	P61255	60S ribosomal protein L26	-0,91	3,96
Ca14	Q9WVT6	Carbonic anhydrase 14	-0,91	2,50
Aacs	Q9D2R0	Acetoacetyl-CoA synthetase	-0,89	4,05
Slc3a2	P10852	4F2 cell-surface antigen heavy chain	-0,88	4,26
Rpl19	A2A547	60S ribosomal protein L19	-0,88	2,53
Slc22a8	O88909	Solute carrier family 22 member 8	-0,82	3,07

Gene names	Uniprot	Protein names	Amino acid (Rap/control)	log$_2$ intensity	-log(p value)	Sequence window	Known site (F	Origin	PhosphoSite	Regulatory sit	Regulatory sit	Regulatory sit	Regulatory sit	Regulatory sit	MOTIF CLASS
Pdzk1	Q9JIL4	Na(+)/H(+) exchange regulatory cofactor NHE-RF3	S148	2,57	5,86	PRLCYLVKEGNSPGPSLKTIQGKKGVYLTDI	+	HTP							BASOPHILIC
Abcc2	Q8VI47	Canalicular multispecific organic anion transporter 1	S906	2,56	1,19	EIPDDAASLTMRRENSLRRTLSRSSRSGSRR	+	HTP							BASOPHILIC
Carhsp1	Q9CR86	Calcium-regulated heat stable protein 1	S53	2,34	0,51	NVVPSPLPTRRTRTFSATVRASQGPVYKGVC	+	CST;HTP							BASOPHILIC
Srrm2	Q8BTI8	Serine/arginine repetitive matrix protein 2	S454	2,28	1,28	LKPTPAPGSRREISSSPTSKNRSHGRAKRDK	+	CST;HTP							PROLINE_DIR
Ndrg1	Q62433	Protein NDRG1	S342	1,69	1,44	RTASGSSVTSLEGTRSRSHTSEGPRSRSHTS	+	CST;HTP							OTHER
Gm8991	E9Q7H5	Heterogeneous nuclear ribonucleoprotein A3	S280	1,49	0,67	YGPMKGGSFGGRSSGSPYGGGYGSGGGSGGY									PROLINE_DIR
Ndrg1	Q62433	Protein NDRG1	T328	1,38	1,40	GYMPSASMTRLMRSRTASGSSVTSLEGTRSR	+	CST;HTP							BASOPHILIC
Dync1h1	Q9JHU4	Cytoplasmic dynein 1 heavy chain 1	S4366	1,38	1,08	DDLAYAETEKKARTDSTSDGRPAWMRTLHTT	+	CST;HTP							BASOPHILIC
Nedd4l	E9PXB7;Q8CFI0	E3 ubiquitin-protein ligase NEDD4-like;E3 ubiquitin-protein ligase	S449	1,12	2,86	NNHLVEPQIRRPRSLSSPTVTLSAPLEGAKD	+	CST;HTP;LTP	SGK1	+	molecular association, regul	14-3-3 beta(INDUCES)			BASOPHILIC
Apon	G3X9D6	Apolipoprotein N, isoform CRA_a	S114	1,12	2,54	GGKDSAETLVLQSQKSSQEEGIGNNEVILRH	+	HTP							ACIDOPHILIC
Apon	G3X9D6	Apolipoprotein N, isoform CRA_a	S115	1,12	2,54	GKDSAETLVLQSQKSSQEEGIGNNEVILRHL	+	HTP							ACIDOPHILIC
Stx7	Q8BH40	Syntaxin-7	S129	1,09	1,85	REKEFVARVRASSRVSGGFPEDSSKEKNLVS									BASOPHILIC
Eps8l2	Q99K30	Epidermal growth factor receptor kinase substrate 8-like protein 2	S17	1,08	1,04	SQSASMSCCPGAANGSLGRSDGVPRMSAKDL									BASOPHILIC
Tns1	A0A087WQS0	Protein Tns1	S1054	1,04	2,31	RQPAEPPGPLRRRAASDGQYENQSPEATSPR									BASOPHILIC
Mme	Q61391	Neprilysin	S4	1,01	2,11	_____MGRSESQMDITDINAPKPK	+	CST;HTP;LTP							ACIDOPHILIC
Aldob	Q91Y97	Fructose-bisphosphate aldolase B	S36	0,99	1,32	QRIVANGKGILAADESVGTMGNRLQRIKVEN	+	HTP							BASOPHILIC
Eif4b	Q8BGD9	Eukaryotic translation initiation factor 4B	S406	0,97	1,85	LDEPKLDRRPRERHPSWRSEETQERERSRTG	+	CST;HTP;LTP		+	translation, altered				BASOPHILIC
Cobll1	B1AZ15	Cordon-bleu protein-like 1	S363	0,97	1,19	VRTGSLQLSSTSIGTSSLKRTKRKAPAPPSK									BASOPHILIC
Ndrg2	Q9QYG0	Protein NDRG2	S350	0,91	1,41	SAASIDGSRSRSRTLSQSSESGTLPSGPPGH	+	CST;HTP							BASOPHILIC
Lmna	P48678	Prelamin-A/C;Lamin-A/C	S404	0,91	2,13	LSPSPTSQRSRGRASSHSSQSQGGGSVTKKR	+	CST;HTP;LTP							BASOPHILIC
Lmna	P48678	Prelamin-A/C;Lamin-A/C	S407	0,91	2,13	SPTSQRSRGRASSHSSQSQGGGSVTKKRKLE	+	CST;HTP;LTP							OTHER
Abcc2	Q8VI47	Canalicular multispecific organic anion transporter 1	S927	0,90	2,36	SRSSRSGSRRGKSLKSSLKIKSVNALNKKEE	+	HTP							BASOPHILIC
Srsf2	Q62093	Serine/arginine-rich splicing factor 2	S26	0,89	3,07	EGMTSLKVDNLTYRTSPDTLRRVFEKYGRVG	+	CST;HTP							PROLINE_DIR
Clmn	Q8C5W0	Calmin	S419	0,88	1,42	ESSILSTRKDGRRSNSLPVKKTVHFEADLHK	+	HTP							BASOPHILIC
Prkd3	Q8K1Y2	Serine/threonine-protein kinase D3;Serine/threonine-protein kinase D	S41	0,84	3,29	PSPCSSPKTGLSARLSNGSFSAPSLTNSRGS	+	HTP							OTHER
Fxyd1	Q9Z239	Phospholemman	S83	0,79	3,88	QRTGEPDEEEGTFRSSIRRLSSRRR_____	+	CST;HTP;LTP		+	intracellular localization			After stimulat	OTHER
Tgfb1i1	E9PYQ1	Transforming growth factor beta-1-induced transcript 1 protein	S341	0,78	2,73	EGRPLCENHPHAQRGSLCATCGLPVTGRCVS									OTHER
Slc4a4	D3Z7G8	Electrogenic sodium bicarbonate cotransporter 1	T3	-2,99	1,15	_____MSTENVEGKPNNLGERGR									ACIDOPHILIC
Srrm2	Q8BTI8	Serine/arginine repetitive matrix protein 2	S1630	-2,58	1,07	PEHAPKSRTARRGSRSSIEPKTKSHTPPRRR	+	HTP							ACIDOPHILIC
Slc7a9	Q9QXA6	B(0,+)-type amino acid transporter 1	S15	-2,25	3,66	_MEETSLRRRREDEKSTHSTELKTTSLQKEV									BASOPHILIC
Slc16a1	P53986	Monocarboxylate transporter 1	S213	-1,86	3,11	IGPEQVKLEKLKSKESLQEAGKSDANTDLIG	+	HTP							ACIDOPHILIC
Slc7a9	Q9QXA6	B(0,+)-type amino acid transporter 1	S18	-1,77	1,71	ETSLRRRREDEKSTHSTELKTTSLQKEVGLL									ACIDOPHILIC
Srrm2	Q8BTI8	Serine/arginine repetitive matrix protein 2	S1631	-1,65	0,95	EHAPKSRTARRGSRSSIEPKTKSHTPPRRRS	+	CST;HTP							ACIDOPHILIC
Slc4a4	A7E1Z5	Electrogenic sodium bicarbonate cotransporter 1	S1060	-1,65	0,62	QQPFLSDNKPLDRERSSTFLERHTSC_____									BASOPHILIC
Slc5a2	Q923I7	Sodium/glucose cotransporter 2	S623 *	-1,39	0,97	RCLLWFCGMSKSGSGSPPPTTEEVAATTRRL	+	HTP							PROLINE_DIR
Rptor	Q8K4Q0	Regulatory-associated protein of mTOR	S722	-1,34	4,04	PVRDSPCTPRLRSVSSYGNIRAVTTARNLNK	+	CST;HTP;LTP							BASOPHILIC
Gbf1	Q6A099	Gbf1 protein	S179	-1,21	2,90	AGGMSDSSKWKKQKRSPRPPRHTTKVTPGSE									PROLINE_DIR
Pdzk1	Q9JIL4	Na(+)/H(+) exchange regulatory cofactor NHE-RF3	S492	-1,20	2,62	PLVAGPDEKGETSAESEHDAHPAKDRTLSTA	+	HTP							ACIDOPHILIC
Wnk4	Q80UE6	Serine/threonine-protein kinase WNK4	S1196	-1,19	2,47	LQRSDLPGPGIMRRNSLSGSSTGSQEQRASK	+	CST;HTP;LTP	SGK1;WNK4						BASOPHILIC
Dcaf8	Q8N7N5	DDB1- and CUL4-associated factor 8	S100	-1,17	5,70	TGHYSINDESRGHGHSDEEDEEQPHRGQRK	+	CST;HTP							ACIDOPHILIC
Ndrg1	Q62433	Protein NDRG1	S330	-1,15	0,86	MPSASMTRLMRSRTASGSSVTSLEGTRSRSH	+	CST;HTP							BASOPHILIC
Rptor	Q8K4Q0	Regulatory-associated protein of mTOR	S863	-1,13	2,81	QRILDTSSLTQSAPASPTNKGMHMHQVGGSP	+	HTP;LTP							PROLINE_DIR
Tns1	A0A087WQS0	Protein Tns1	S1067	-1,12	1,45	AASDGQYENQSPEATSPRSPGVRSPVQCVSP									PROLINE_DIR
Tra2b	P62996	Transformer-2 protein homolog beta	S95	-1,12	0,78	RSRSRSYSRDYRRRHSHSHSPMSTRRRHVGN	+	CST;HTP							BASOPHILIC
Tra2b	P62996	Transformer-2 protein homolog beta	S99	-1,12	0,78	RSYSRDYRRRHSHSHSPMSTRRRHVGNRANP	+	CST;HTP							PROLINE_DIR
4833439L19Rik	D3Z1F7	Putative monooxygenase p33MONOX	S164	-1,11	1,24	HPASAQSTPSSTPHASPKQKSRGWFPSGSST									PROLINE_DIR
Lrp2	A2ARV4	Low-density lipoprotein receptor-related protein 2	S4577	-1,09	2,95	RSIDPSEIVPEPKPASPGADETQGTKWNIFK	+	HTP							PROLINE_DIR
Dennd5b	A2RSQ0	DENN domain-containing protein 5B	S1068	-1,08	2,87	DEDLGKQCRTPPQQKSPTTTRRLSITSLTGK	+	HTP							PROLINE_DIR
Dennd5b	A2RSQ0	DENN domain-containing protein 5B	T1062	-1,08	2,87	LMTSASDEDLGKQCRTPPQQKSPTTTRRLSI	+	HTP							PROLINE_DIR
Hsp90aa1	P07901	Heat shock protein HSP 90-alpha	S231	-1,07	3,00	YPITLFVEKERDKEVSDDEAEEKEEKEEEKE	+	CST;HTP							ACIDOPHILIC
Erc1	V9GWT6	ELKS/Rab6-interacting/CAST family member 1	S21	-1,05	1,40	RSVGKVEPSSQSPGRSPRLPRSPRLGHRRTN									PROLINE_DIR
Smarcc1	P97496	SWI/SNF complex subunit SMARCC1	S309	-1,04	3,30	SFRQRISTKNEEPVRSPERRDRKASANSRKR	+	HTP							PROLINE_DIR
Slc4a4	A7E1Z5	Electrogenic sodium bicarbonate cotransporter 1	S232	-0,98	1,44	KKSNLRSLADIGKTVSSASSPAMTHRNLTSS	+	CST;HTP							BASOPHILIC
Matr3	Q8K310	Matrin-3	S604	-0,93	1,17	KDKSRKRSYSPDGKESPSDKKSKTDAQKTES	+	CST;HTP							PROLINE_DIR
Rbm14	Q8C2Q3	RNA-binding protein 14;RNA-binding protein 4B;RNA-binding protein 4	S215	-0,92	3,54	GQARQPTPPFFGRDRSPLRRSPPRASYVAPL	+	HTP							PROLINE_DIR
Srsf2	Q62093	Serine/arginine-rich splicing factor 2	S189	-0,91	3,54	SSVSRSRSRSRSRSRSRSPPPVSKRESKSRS	+	HTP							BASOPHILIC
Srsf2	Q62093	Serine/arginine-rich splicing factor 2	S191	-0,91	3,54	VSRSRSRSRSRSRSRSPPPVSKRESKSRSRS	+	HTP							PROLINE_DIR
Kiaa1468	A0A087WSS1	LisH domain and HEAT repeat-containing protein KIAA1468	S193	-0,90	2,29	AGSISTLDSLDFARYSDDGNRETDERVAEHE									ACIDOPHILIC
Ybx1	P62960	Nuclease-sensitive element-binding protein 1	S172	-0,84	2,87	QQNYQNSESGEKNEGSESAPEGQAQQRRPYR	+	CST;HTP							ACIDOPHILIC
Thrap3	Q569Z6	Thyroid hormone receptor-associated protein 3	S669	-0,82	2,16	YLKRGNEQEAAKNKKSPEIHRRIDISPSTFR	+	CST;HTP							PROLINE_DIR
Mapt	P10637	Microtubule-associated protein tau	S527	-0,79	2,33	TREPKKVAVVRTPPKSPSASKSRLQTAPVPM	+	CST;HTP;LTP							PROLINE_DIR
Arvcf	P98203	Armadillo repeat protein deleted in velo-cardio-facial syndrome homolog	S345	-0,78	2,29	PERGSLGSLDRVVRRSPSVDSTRKEPRWRDP	+	HTP							PROLINE_DIR
Epb4.1l1	A2AUK8;E9PV14	Band 4.1-like protein 1	S461	-0,78	2,60	HDAGPDGDKREDDAESGGRRSEAEEGEVRTP	+	HTP							OTHERH
Epb4.1l1	A2AUK8;E9PV14	Band 4.1-like protein 1	S466	-0,77	2,86	DGDKREDDAESGGRRSEAEEGEVRTPTKIKE									ACIDOPHILIC
Dennd5b	A2RSQ0	DENN domain-containing protein 5B	S178	-0,76	3,19	DEGDATSLLKLQRYNSYDINRDTLYVSKSIC	+	CST;HTP							BASOPHILIC

* Valid intensity values for this site only in 5 control and 4 Rap animals (missing value in 1 Rap animal)